

Mean Wind in Convective Turbulence of Mercury

Yoshiyuki Tsuji,¹ Takatoshi Mizuno,¹ Takashi Mashiko,² and Masaki Sano²

¹*Department of Energy Engineering and Science, Nagoya University, Nagoya 464-8603, Japan*

²*Department of Physics, University of Tokyo, Tokyo 113-0033, Japan*

(Received 18 June 2004; published 26 January 2005)

The large-scale circulation, often called “wind,” in the confined thermal turbulence of mercury is studied experimentally. The instantaneous velocity profile at 128 points is directly measured using ultrasonic velocimetry. The periodic velocity oscillation is observed in the case of the aspect-ratio $\Gamma = 1, 2$ but not in $\Gamma = 0.5$. Its peak frequency is scaled by $f_c \propto \text{Ra}^{\gamma_c}$, where Ra is the Rayleigh number and $\gamma_c = 0.43, 0.45$ for $\Gamma = 1, 2$. f_c is close to the wind circulation frequency f_p , and has the same order of transit time from the bottom to the top of the convection cell. A single roll circulation is expected in $\Gamma = 1$; however, axisymmetric toroidal rings may exist near the upper and lower plate for $\Gamma = 0.5$, which are stable up to $\text{Ra} = 7 \times 10^{10}$.

DOI: 10.1103/PhysRevLett.94.034501

PACS numbers: 47.27.Te

Thermal convection has been a subject of long standing interest and has many applications in science and engineering. Heat transport problems are also frequently encountered in technological applications. One of the recurrent themes of confined thermal turbulence in the Rayleigh-Bénard apparatus is the relation between a large-scale circulation, which is often called “wind,” and a plume emitted from top or bottom walls. The wind survives even when the dynamic parameter, Rayleigh number Ra , is very large [1]. The thermal plumes generated close to the wall are carried away by the constant wind. A periodic oscillation of temperature associated with passing plumes has been observed close to the sidewall. The peak frequency f_p [Hz], or $\omega_p = 2\pi f_p$, of temperature fluctuation is well scaled by the Rayleigh number as a power-law relation; $f_p \propto \text{Ra}^{\gamma_p}$. The exponent γ_p may depend on an aspect ratio of the cell and the Prandtl number of the working fluid [2–5]. The mean wind velocity U_w has a simple relation to f_p as $U_w \simeq \ell f_p$, where ℓ is a circulation path of wind. For example, in aspect ratio one cell, ℓ is equal to four times the cell height L . The relation $f_p \simeq U_w/(4L)$ is assumed if the wind is steady. This relation has been ascertained by several researchers [1,2,4,6], and a physical model was presented by Villermaux [7].

The mean wind speed U_w is evaluated based on the temperature fluctuation measured at two points with a small separation distance Δd in the vertical direction [2]. If the convective motion consists of mean wind and periodic modulation caused by plumes, the temperature signals from the sensors would be identical to evaluate the mean wind speed. When the two-point temperature correlation indicates its maximum at a time lag Δt , the mean wind is given by $U_w = \Delta d/\Delta t$. Noting that Δt could be positive or negative, one is upward flow and the other is downward. A recent experiment shows that the wind direction reverses occasionally but is not periodic [1]. Why does the wind direction reverse? Is the wind circulation quasi-two-dimensional, or is it really steady? Is there any aspect-ratio

dependence? We still have many questions about the flow patterns in a confined cell. This is because the velocity information has been almost completely limited to the mean wind speed U_w at one location in space, and the instantaneous velocity profile was not directly monitored. Direct velocity measurement is important to reveal the wind circulation. However, in contrast to the great number of temperature measurements, experimental information on velocity is rather limited. Qiu and Tong [8] reviewed the velocity measurements in thermal convection, and they also obtained the velocity information by a laser Doppler velocimetry (LDV) system. Burr *et al.* [9] applied the particle image velocimetry (PIV) technique and the two-dimensional velocity field was analyzed. Both LDV and PIV are conventional methods but they are only applicable to transparent fluid. There are few attempts to measure the velocity of liquid metal. Mashiko *et al.* [10] utilized ultrasonic velocimetry and measured the instantaneous velocity profile. They analyzed statistical quantities such as the wave-number spectrum, time-frequency spectrum, and probability density function. The usefulness of this technique has been confirmed.

In this study, utilizing the ultrasonic velocimetry, we measure the instantaneous velocity at 128 points on the center line of a cell. The working fluid used is mercury, whose Prandtl number is about 0.024. Although the wind seems to be constant and quasi-two-dimensional during a long period, it might be affected by plumes. If so, the circulation pattern should vary instantaneously. This point is discussed and its aspect-ratio dependence is studied in this Letter. In mercury, the strong evidence that the viscous boundary layer is nested inside the thermal boundary layer has been provided. However, this condition is essentially different from that of experiments at higher Pr number [11]. The direct velocity measurement will reveal some new information for this problem.

Figure 1 shows a schematic drawing of the convection cell, which is a vertical cylinder with its inner diameter and height being $D = 10$ and $L = 5, 10, 20$ cm, respectively

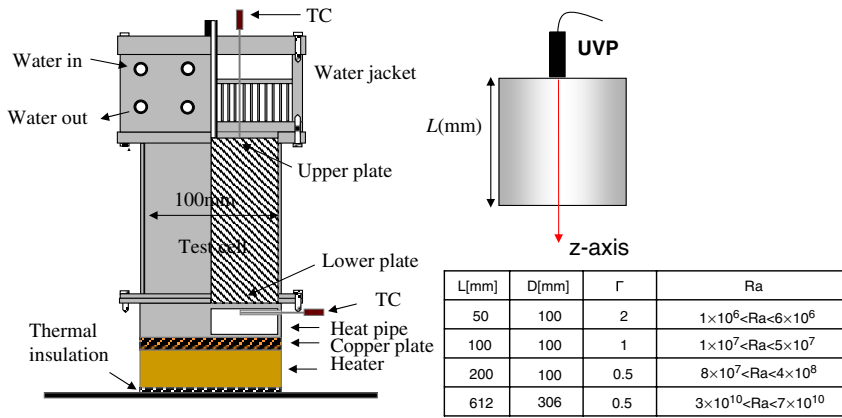


FIG. 1 (color online). Schematic view of experimental apparatus and coordinate system.

(the aspect ratio $\Gamma \equiv D/L$ is thus 2, 1, 0.5). The sidewall, upper, and lower plates are made of stainless steel. The temperature of the upper plate is regulated by passing cold water through a cooling chamber fitted on the top of the plate. The lower plate is heated uniformly at a constant rate with a heat pipe. The temperature difference ΔT between the two plates is measured by a thermocouple imbedded inside the plates. One of the dominant control parameters in this experiment is the Rayleigh number. It is a function of the temperature difference between the upper and bottom plates ΔT , and is defined as $Ra \equiv \alpha \Delta T g L^3 / \nu \kappa$ with g being the gravitational acceleration, L the height of the cell, and α , ν , and κ being the thermal expansion coefficient, the kinematic viscosity, and the thermal diffusivity, respectively. During our experiment, only the bottom temperature is changed, so the average temperature of mercury at the center is not constant. Ra is changed from 10^6 to 4×10^8 and its relation to the Nusselt number, Nu , is $Nu = 0.095 \times Ra^{0.294}$. This is similar to the result of Takeshita *et al.* [4], Cioni *et al.* [6], and Glazier *et al.* [12]. We also performed another experiment using a large-scale cell whose diameter, height, and aspect ratio are 30.6 cm, 61.2 cm, and $\Gamma = 0.5$, respectively. The Rayleigh number is up to 7×10^{10} . Detailed experimental conditions were reported previously [10].

An ultrasonic velocity profile (UVP) meter measures an instantaneous velocity profile of liquid flows based on the Doppler shift frequency in echoes reflected by small passive particles in liquid. The principle of UVP is based on the echography for the measurement of location and the Doppler shift relationships for the measurement of velocity [13,14]. The UVP transducer emits an ultrasonic pulse at a frequency of 4 MHz and receives reflected echoes over a time interval between consecutive pulse emissions. Instantaneous velocities are obtained at 128 locations along the path of ultrasonic pulses. The particle locations are known from the time lag of the echo behind the pulse emission.

A piezoelectric, ultrasonic transducer, 5 mm in diameter and 6 cm in length, is mounted on the top of the outer surface (Fig. 1). The velocity is measured simultaneously

at 128 points 0.74 mm apart from each other on the center line of the cell. The vertical axis is z and its origin is at the upper plate. The velocity is defined as positive in $+z$ direction and negative for $-z$. The data are sampled every 0.132 s. The velocity resolution is about 0.7 mm/s under this condition. The sampling volume, or the space resolution, is the shape of a disk whose diameter is 5 mm and thickness is 0.74 mm.

Figure 2 shows the frequency spectra of velocity at the cell center. There is a peak frequency f_c in the cases of aspect ratios 1 and 2, but not at $\Gamma = 0.5$. Then the velocity oscillates in some periodic mode depending on the Rayleigh number. Does this frequency f_c relate to the period of plume emission? Plume shedding frequency f_p , usually called a rotation frequency based on temperature fluctuation, indicates the simple power-law relation $2\pi f_p L^2 / \kappa = CRa^{\gamma_p}$. Naert *et al.* obtained $\gamma_p = 0.4 \pm 0.04$ for $\Gamma = 2$ cell and 0.44 ± 0.02 for $\Gamma = 1$ [11]. Similar results were reported by [4,6,15]. In the present experiment, f_c can also be scaled by the relation $2\pi f_c L^2 / \kappa = C'Ra^{\gamma_c}$. The exponents are $\gamma_c = 0.43$ and

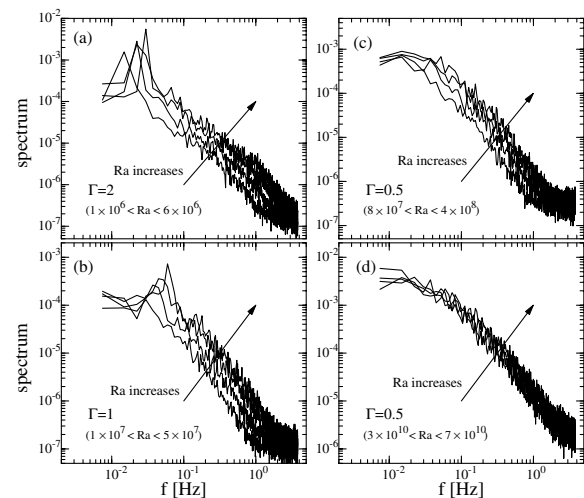


FIG. 2. Typical example of frequency spectra measured at the cell center. (a) $\Gamma = 2$, (b) $\Gamma = 1$, (c) $\Gamma = 0.5$, and (d) $\Gamma = 0.5$, (large cell). Peak frequency is defined as f_c .

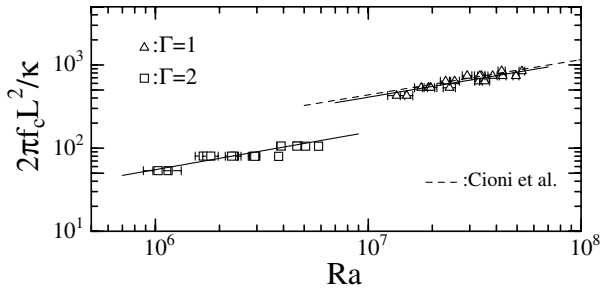


FIG. 3. Normalized peak frequency of velocity fluctuation f_c at the cell center. The dashed line indicates the rotational frequency f_p by Cioni *et al.* [6].

0.45 for $\Gamma = 1$ and 2, respectively, as plotted in Fig. 3. The aspect-ratio dependence will be discussed later. It is not necessary to coincide with each other, but compared with the results of Cioni *et al.* (see dashed line in Fig. 3), the difference between present f_c and f_p by Cioni *et al.* is very small. Based on these experimental results, we assume that velocity oscillation is not confined at the cell center, but plume emission from top or bottom plates has a significant effect on it. Qiu *et al.* observed a similar trend in an aspect ratio of one cell filled with water at $10^9 \leq Ra \leq 10^{10}$ [5]. The velocity component in both horizontal directions exhibited oscillation, but not in the vertical direction, whose scaling exponent is 0.43 ± 0.06 . This value is the same as that of f_p , and they concluded the oscillation is the response of the bulk fluid to the horizontal perturbations produced by the warm and cold plumes near the sidewall. Also, Segawa *et al.* found temperature oscillation at the cell center at $\Gamma = 2$.

Analogous with $f_p \approx U_w/(4L)$ [2], we consider the relation between f_c and the mean velocity. The upward and downward mean velocity at the cell center are defined as U^+ and U^- , respectively. The absolute values of these are equal, and we represent it as $U_c \equiv |U^+| = |U^-|$. Compared to the free fall velocity $U_F \equiv (\alpha \Delta T g L)^{1/2}$, U_c/U_F is approximately 0.5 for $\Gamma = 2$ and 0.1 for $\Gamma = 1$, but is a slightly decreasing function of Ra . In Fig. 4, the peak frequency f_c is normalized by U_c and D . Here, D is the cell diameter. The ratio $f_c D/U_c \approx 1$ for $\Gamma = 1$ and ≈ 0.5 for $\Gamma = 2$ is independent of the Rayleigh number. Therefore, we have a simple relation like $4f_p/U_w \approx$

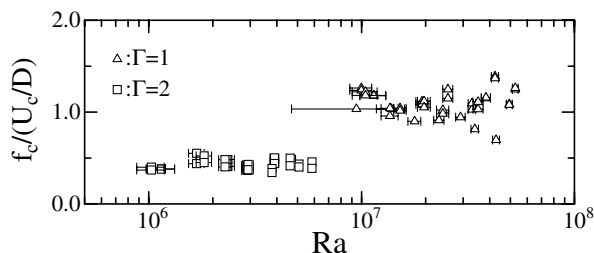


FIG. 4. Peak frequency is normalized by D and U_c . U_c is a mean upward (or downward) velocity at the cell center, and D is a cell diameter.

f_c/U_c for $\Gamma = 1$. It is not necessary for U_c to be U_w or that f_p matches f_c . As pointed out by Villiermaux, if the oscillation results from the delayed coupling of the boundary layer instabilities by the slow convective motion of the circulation, there is a time lag τ , which is the transit time from the bottom to the top of the convection cell [7]. The oscillation frequency is essentially proportional to the inverse of τ . Here, τ is assumed to be L/U_c and then oscillation occurs at a frequency of U_c/L . This is well satisfied in our experiment for $\Gamma = 1$.

In Fig. 5 we show the instantaneous velocity distribution. The vertical axis is the distance from the upper wall, and the horizontal axis indicates time. We only monitor the vertical component of velocity on the center line of the cell. Positive and negative signs indicate the downward and upward velocity, respectively. The origin of the z axis is set at the upper plate. Velocity fluctuations are classified into eight levels between the maximum and minimum values, and they are identified each in its own color. In the case of $\Gamma = 2$, the downward and upward flow oscillate in opposition of phase. The flow from the bottom goes through the cell and reaches the top, and vice versa. Coherent motion is comparable to the cell height L . The average velocity distribution along the z axis, $U(z)$, is approximately zero as plotted in Fig. 5. The cell-center velocity changes its sign periodically, and this makes for a sharp peak in the frequency spectrum (see Fig. 2). The flow from the bottom wall does not always reach the opposite plate for $\Gamma = 1$. Around the top plate, the downward flow is dominant, and the upward flow sweeping the bottom reaches occasionally. This makes $U(z)$ positive at $0 < z/L < 1/2$ and negative at $1/2 < z/L < 1$. At the cell center we can observe the periodic change of the velocity direction, but it is not as clear as at $\Gamma = 2$. This observation is consistent with finding that the spectral peak is not so sharp at $\Gamma = 1$ as at $\Gamma = 2$, and the normalized frequencies $2\pi f_c L^2/\kappa$ differ slightly as plotted in Fig. 3. This might be because the flow pattern or the wind differs depending on the aspect ratio.

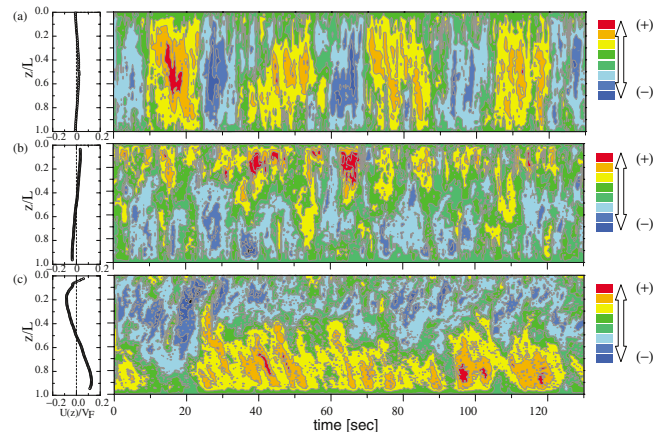


FIG. 5 (color). Contour of instantaneous velocity fluctuation on the center line of the cell. (a) $\Gamma = 2$, (b) $\Gamma = 1$, and (c) $\Gamma = 0.5$.

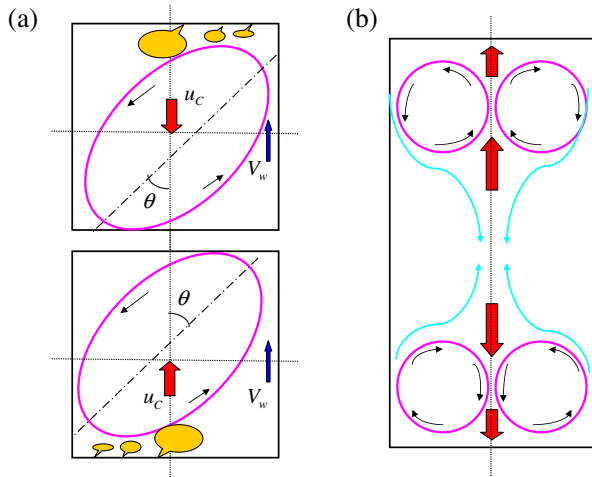


FIG. 6 (color online). (a) Elliptical flow pattern of $\Gamma = 1$ which departs from the z axis with an angle of θ . When bottom (top) plumes are active, upward (downward) velocity u_c is observed at the cell center. V_w is the mean velocity at the sidewall. (b) Flow pattern of $\Gamma = 0.5$. Axisymmetric toroidal rings exist steadily near the upper and lower plates. The mean velocity direction on the z axis is indicated by thick arrows.

Periodic oscillation is not observed at $\Gamma = 0.5$. This is clearly shown in the time-frequency spectrum in Fig. 2. As indicated in the contour map Fig. 5(c), the upward flow is dominant around the top plate and the downward flow is stationary over the bottom plate. The flow sweeping the bottom (top) plate hardly reaches the top (bottom) plate. Then $U(z)$ is negative at $0 < z/L < 1/2$ and becomes positive at $1/2 < z/L < 1$. Thus, the distribution is opposite that of $\Gamma = 1$. It is also noted that the contour map is slightly tilted. In the lower half region ($1/2 \leq z/L \leq 1$), the contour has a negative slope. This means that a lump of fluid goes down on the center line with almost steady velocity. In the upper half region ($0 \leq z/L \leq 1/2$), the opposite motion, going upward on the center line, is ascertained.

To summarize, we conclude that the wind is across the z axis in the case of $\Gamma = 1$. This provides an elliptical pattern whose axis departs from the z axis with an angle of θ [Fig. 6(a)] [8,16]. However, θ should fluctuate rather than be constant. If the upper region is populated by plumes, the wind circulation shifts down and the downward velocity is monitored at the cell center. When the plumes from the lower plate become strong, upward velocity is observed at the cell center. They are repeated alternatively. The time lag between these two states is $\tau \approx L/U_c$, and the frequency peak is given by $f_c \approx 1/\tau$. Here, the frequency f_c is close to f_p , and the wind circulation is not steady. This is the process of velocity oscillation observed in this experiment. The mean velocity at the sidewall V_w is constant even if these oscillations occur. When the flow pattern rotates in the azimuthal direction, V_w reverses. However, we still have little information about

the origin of azimuthal rotation and the reverse period of V_w [17].

The flow pattern of $\Gamma = 0.5$ is shown in Fig. 6(b). Following the discussion of the contour map in Fig. 5(c), a lump of fluid moves on the center line. It goes upward in the upper half region and downward in the lower half. This makes us imagine that the axisymmetric toroidal rings exist steadily near the upper and lower plates [10,18]. The tilted contour map has been observed up to $Ra = 7 \times 10^{10}$. At the cell center, the upward and downward flow exist alternatively, but they are not periodic. So the coupling between the top and bottom plumes is little [19]. In the case of $\Gamma = 2$, the present experimental results are not enough to have a clear image of the flow pattern. As the mean velocity profile is approximately zero along the z axis, a symmetrical roll may dominate in the cell. However, the normalized oscillation frequency $f_c L/U_c$, its Rayleigh number dependence, and the contour velocity map are different from those of $\Gamma = 1$, where the wind circulation and its azimuthal rotation are affected by plume shedding in a different way. These are forthcoming studies.

- [1] J.J. Niemela, L. Skrbek, K.R. Sreenivasan, and R.J. Donnelly, *J. Fluid Mech.* **449**, 169 (2001).
- [2] M. Sano, X.Z. Wu, and A. Libchaber, *Phys. Rev. A* **40**, 6421 (1989).
- [3] B. Castaing, G. Gunaratne, F. Heslot, L. Kadanoff, A. Libchaber, S. Thomae, X.-Z. Wu, S. Zaleski, and G. Zanetti, *J. Fluid Mech.* **204**, 1 (1989).
- [4] T. Takeshita, T. Segawa, J. A. Glazier, and M. Sano, *Phys. Rev. Lett.* **76**, 1465 (1996).
- [5] X.-L. Qiu, S. H. Yao, and P. Tong, *Phys. Rev. E*, **61**, R6075 (2000).
- [6] S. Cioni, S. Ciliberto, and J. Sommeria, *J. Fluid Mech.* **335**, 111 (1997).
- [7] E. Villermaux, *Phys. Rev. Lett.* **75**, 4618 (1995).
- [8] X.-L. Qiu and P. Tong, *Phys. Rev. E* **64**, 036304 (2001).
- [9] U. Burr, W. Kinzelbach, and A. Tsinober, *Phys. Fluids* **15**, 2313 (2003).
- [10] T. Mashiko, Y. Tsuji, T. Mizuno, and M. Sano, *Phys. Rev. E* **69**, 036306 (2004).
- [11] A. Naert, T. Segawa, and M. Sano, *Phys. Rev. E* **56**, R1302 (1997).
- [12] J. A. Glazier, T. Segawa, A. Naert, and M. Sano, *Nature (London)* **398**, 307 (1999).
- [13] Y. Takeda, *Int. J. Heat Mass Flow* **7**, 313 (1986).
- [14] T. Ito, Y. Tsuji, and Y. Kukita, *Exp. Fluids* **31**, 324 (2001).
- [15] R. Camussi and R. Verzicco, *Phys. Fluids* **10**, 516 (1998).
- [16] L. P. Kadanoff, *New Perspectives in Turbulence* (Springer-Verlag, Berlin, 1991), pp. 263–269.
- [17] K. R. Sreenivasan, A. Bershadskii, and J. J. Niemela, *Phys. Rev. E* **65**, 056306 (2003).
- [18] R. Verzicco and R. Camussi, *J. Fluid Mech.* **477**, 19 (2003).
- [19] It is also noted that one role cell is another candidate for $\Gamma = 0.5$ [8,10]. This will be discussed in the future work.